AFM studies of Pd silica supported thin film catalysts

Kong Hean Lee and Eduardo E. Wolf[1]

Department of Chemical Engineering, University of Notre Dame, Notre Dame, IN 46556, USA

Received 9 November 1993; accepted 23 March 1994

AFM has been used to study the effects of pretreatment gases on Pd/SiO_2 supported thin film catalysts during 1,3-butadiene hydrogenation. The Pd/SiO_2 catalyst, treated with O_2 followed by H_2 at 450°C, has an initial conversion of 85% and a surface morphology of 60×65 nm^2 Pd grains and only deactivates slightly. After a second treatment, the reactivity was fully recovered and the surface morphology exhibits a redispersion of the Pd grains. The catalyst with a similar initial reactivity and morphology but only treated in H_2, shows a decrease in activity and coalescence of Pd grains after repeated treatment. XPS studies have shown that the O_2 and H_2 treated Pd/SiO_2 catalyst has a lower Pd binding energy than the H_2 treated Pd/SiO_2. The effect of the substrate thickness and composition is also reported.

Keywords: AFM; STM; XPS; Pd thin film; pretreatment effect; 1,3-butadiene hydrogenation

1. Introduction

The atomic force microscope (AFM) has become an important surface characterization tool in many areas of scientific research since its invention by Binnig et al. [1] in 1986. The AFM, capable of imaging non-conductive materials, has become a complementary tool to the scanning tunneling microscope (STM), which is limited to imaging conductive surfaces. While in principle both STM and AFM can help in elucidating catalyst microstructures, there are only a few STM [2–10] and AFM [2,3] applications devoted to the study of supported catalyst particles.

Previous STM work in our group has focused on the study of H_2 pretreatment and reaction on Pd supported catalysts [6,9] and Pd thin films supported on graphite [5,10]. Thus, it was not possible to study the effect of O_2 pretreatment on graphite supports since it leads to carbon gasification [2]. The AFM affords the utilization of other supports that permit the investigation of morphological and compositional effects induced by O_2 treatment which have been shown to affect the catalytic activity of other noble metals [11,13,14]. The reaction studied is 1,3-butadiene hydrogenation due to its high reactivity on low-surface area Pd catalysts and its

[1] To whom correspondence must be addressed.

well-studied mechanism [15–17]. X-ray photoelectron spectroscopy (XPS) was used to determine surface composition.

2. Experimental

2.1. THIN FILM PREPARATION

Two types of thin film catalysts were prepared on different silica substrates: (a) a 200 nm SiO_2 layer grown on a Si wafer (Technology Corp., P-(100)) by oxidizing it in a dry oxygen atmosphere at 1100°C for 3 h and (b) a 500 μm thick SiO_2 wafer (American Si Products, N-(100)). The first support is referred as SiO_2/Si and the second as SiO_2. A thin film Pd catalyst was prepared by evaporating 15.7 mg (corresponding to 14 nm film thickness according to the calibration curve of the evaporator and was further confirmed by STM by measuring the line scans at the edges of the sample or by measuring through rifts which show the exposed substrates) of a Pd wire (Johnson Matthey, 99.997%) at 1×10^{-6} Torr in a vacuum evaporator (Denton DV-502) onto either substrate.

For each substrate, fourteen samples (0.75 cm^2 each) were placed in a 30° tilted platform in the vacuum evaporator to allow uniform Pd deposition. Two new pieces of film catalysts (1.5 cm^2 total area) were used in each activity study, kinetic measurement, AFM study, and XPS analysis.

2.2. ACTIVITY MEASUREMENT

1,3-butadiene hydrogenation was chosen as a probe reaction. The four major products of 1,3-butadiene hydrogenation, namely 1-butene, *n*-butane, cis- and trans-2-butene were monitored to study the pretreatment effect on the selectivity.

Two pieces of film catalysts were placed in a 0.8 cm quartz tube reactor and were pretreated at 450°C, either in H_2 for 8 h or in O_2 followed by H_2 for 4 h each. A 1 h long reaction was carried out after the pretreatment. The catalyst was then treated and reacted again without exposure to air. The reactive mixture consists of 1,3-butadiene (Matheson Gas Products), hydrogen, and nitrogen (UHP grade, Mittler supply corp.). The partial pressure of butadiene is 4 Torr. With a hydrogen-to-butadiene ratio of 125 and nitrogen as diluent, the overall gas flowrate is 115 ml/min at 1 atm. The high hydrogen-to-butadiene ratio was used to reduce carbon deposition and hence to minimize catalyst deactivation. The reaction products were separated in a gas chromatograph, equipped with a 7 ft chromatographic column packed with 0.19% picric acid/graphpac packings (Alltech Associates, Inc) and a FID detector.

The activity of each catalyst with different treatment history was compared at 100°C. The selectivity versus conversion measurements were accomplished by varying the temperature of the reactor. During kinetics measurements, the conversion was kept below 20%.

2.3. ATOMIC FORCE MICROSCOPY (AFM)

The AFM used in this study is a commercial Nanoscope II system (Digital Instrument Inc.) operated at ambient conditions. Two AFM scan heads (700 nm range and 8000 nm range) with silicon nitride probes were employed. The AFM tips were examined repeatedly with mica to ensure the sharpness of the tip and to prevent any tip effects. After treatment and reaction, the Pd film catalyst was taken out of the reactor and imaged with the AFM to examine the catalyst morphological transformation. The AFM was operated in the height imaging mode and at low scan frequency (<2 Hz) to ensure good image resolution and to yield reasonable morphological information. The effect of the pretreatments was also studied by AFM on both SiO_2/Si and SiO_2 substrates without Pd. It was found that the surfaces of both substrates are very smooth with a roughness of approximately <1 nm. Treatments in H_2 and O_2–H_2 did not alter the roughness, morphology, or composition of the films without Pd. As a result, the corresponding featureless micrographs are not shown. The subsequent changes observed after each treatment and reaction, hence are induced by the Pd layer. Four areas from each piece of catalysts were imaged after each reaction to obtain unbiased surface microstructures. The scan sizes were varied from 100×100 nm^2 to 4000×4000 nm^2 to collect small scale structure as well as long range surface order. The images shown here are representative of the sample surface morphology imaged after reaction. The grain measurements are reported as the major and minor axis of an ellipse and are the averages of about 100 particles.

2.4. X-RAY PHOTOELECTRON SPECTROSCOPY (XPS)

The XPS experiments were performed in a spectrometer from Katos Analytical Inc., using monochromatic Mg Kα radiation ($h\nu = 1253.6$ eV). The base pressure of the instrument was 1×10^{-9} Torr. The electron binding energy scale was calibrated by assigning 284.6 eV to the C 1s peak position. The samples were exposed to air while being transferred from the reactor to the XPS chamber. Pitchon et al. [18] have shown via XPS that Pd/SiO_2 catalysts exposed to ambient-conditions exhibited no measurable surface oxidation, an effect confirmed by our measurements.

3. Results and discussion

3.1. $Pd/SiO_2/Si$ THIN FILM CATALYST

To investigate the effect of pretreatment gases on $Pd/SiO_2/Si$ film catalyst, two pieces (1.5 cm^2 total) were pretreated in H_2 for 8 h, while the other two were pretreated in O_2 followed by H_2 for 4 h each at 450°C respectively. After the pretreatment, the catalysts were cooled down to 100°C. The hydrogenation of 1,3-butadiene was carried out at 100°C and the effluent gases were monitored for 1 h.

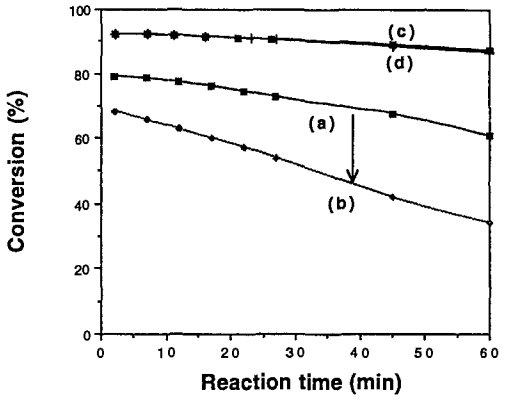

Fig. 1. The conversion of 1,3-butadiene hydrogenation over $Pd/SiO_2/Si$. (a) 8 h H_2 treated fresh film, (b) 8 h H_2 regenerated film, (c) 4 h O_2 + 4 h H_2 fresh film, (d) 4 h O_2 + 4 h H_2 regenerated film.

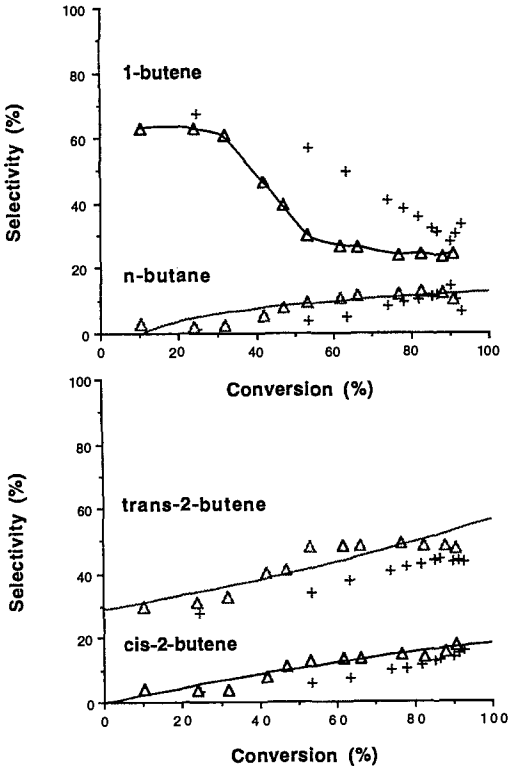

Fig. 2. The selectivity plot of 1,3-butadiene hydrogenation over $Pd/SiO_2/Si$. ((△) H_2 treated sample, (+) O_2 + H_2 treated sample, selectivity plots of H_2 treated catalyst were interpolated.)

After the reaction, the used catalysts were immediately heated up to 450°C and regenerated in the same gases and conditions as the fresh catalysts. The activity was measured again at 100°C for 1 h.

Fig. 1a shows that the H_2 treated Pd catalyst has an initial conversion of 78% and deactivates by more than 15% after 1 h of reaction. The second H_2 treatment did not completely recover the initial catalyst activity, and the initial 68% conversion dropped to 34% after 1 h of reaction (fig. 1b). In contrast, when a fresh catalyst was treated in the O_2 and H_2 treatment, the initial conversion of 1,3-butadiene was about 92% and the catalyst exhibited only a slight deactivation (fig. 1c). The second O_2–H_2 treatment completely restored the catalyst activity (fig. 1d). Fig. 2 features the selectivity plots of 1,3-butadiene hydrogenation on $Pd/SiO_2/Si$. The 1-butene selectivity of the H_2 treated $Pd/SiO_2/Si$ catalyst shows a more drastic decrease at lower conversion than that of O_2 and H_2 treated catalyst. The *n*-butane selectivity increases with conversion, corresponding slightly to the decreasing of 1-butene selectivity. The cis- and trans-2-butene selectivities increase with increasing conversion.

Due to the thin film nature of both $Pd/SiO_2/Si$ catalysts, its initial microstructures can be examined by AFM. The images of the initial $Pd/SiO_2/Si$ catalyst obtained from both microscopes show flat film-like surface features. Better resolution of the initial $Pd/SiO_2/Si$ film obtained by STM (fig. 3) shows a surface of clo-

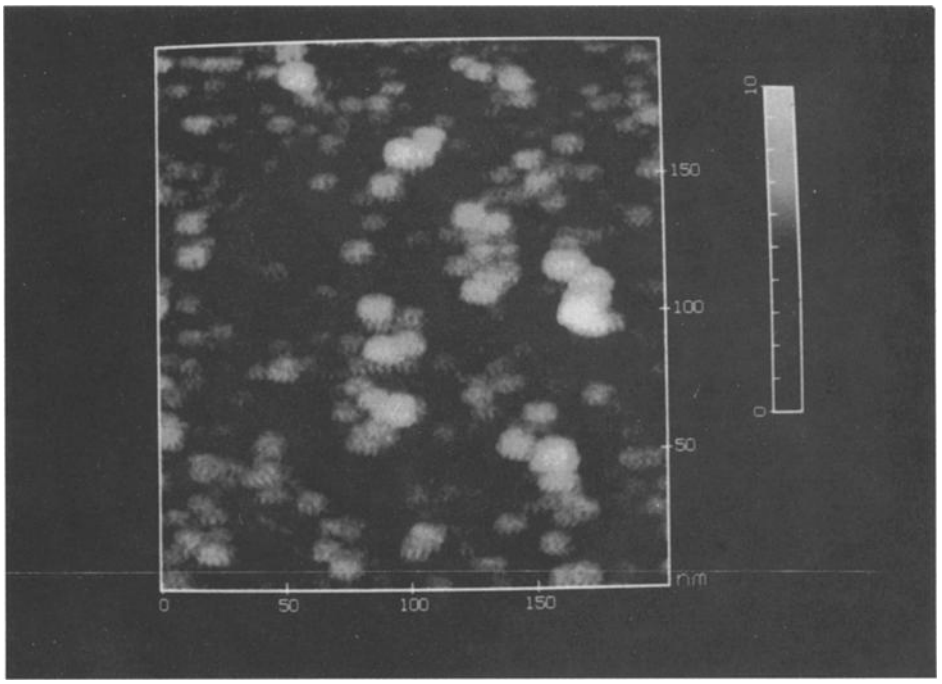

Fig. 3. STM image of initial $Pd/SiO_2/Si$ film structure, 200 × 200 nm.

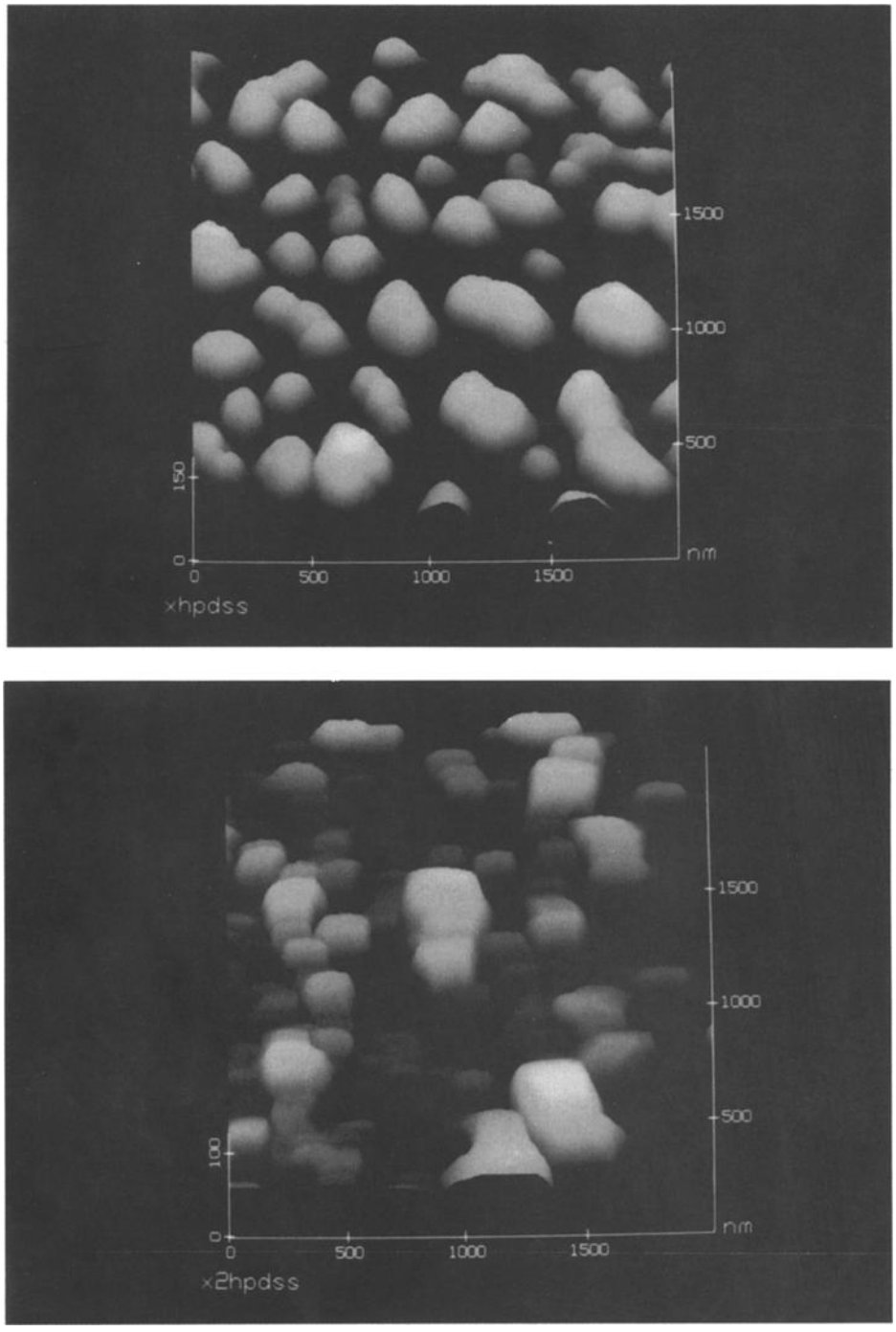

Fig. 4. AFM images of $Pd/SiO_2/Si$ film catalyst after reaction. (2000×2000 nm^2) (a) 8 h H_2 treated fresh film, (b) 8 h H_2 regenerated film, (c) 4 h O_2 + 4 h H_2 fresh film, (d) 4 h O_2 + 4 h H_2 regenerated film.

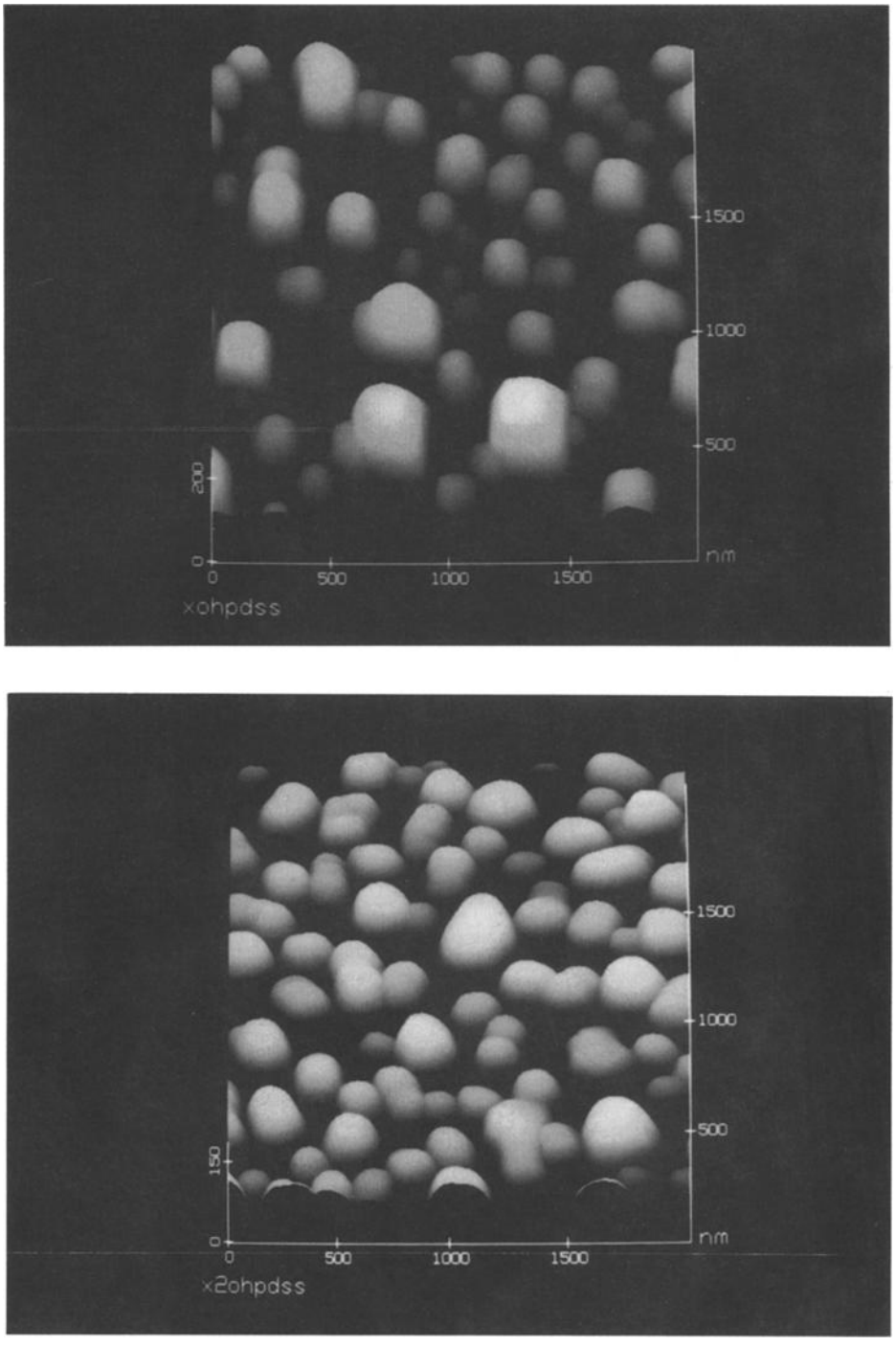

Fig. 4. Continued.

sely packed 14 nm Pd grains with occasion rifts that exposed the substrate layer. After pretreatments and reactions, the coalescence of the grains results in further breakage of the film exposing more of the substrate. The XPS results show a low intensity Si 2p peak for the fresh film. The Si 2p signal intensity increases as the film is subjected to the various treatments. No STM results were obtained on the partially ruptured films due to the poor conductivity of the SiO_2 substrates.

AFM images obtained after H_2 or O_2–H_2 treatment and 1 h of reaction are displayed in fig. 4, showing a scan area of 2000 × 2000 nm^2. After 8 h of H_2 treatment, the reacted $Pd/SiO_2/Si$ film (fig. 4a) shows sintering and coalescence of grains scattered on the surface from the initial 14 nm grains to sizes ranging from 100 × 230 to 240 × 400 nm. The average thickness of the grains is about 65 nm, which is much greater than that of the Pd films initially deposited. We concluded that the grains imaged represent both Pd and partial sintering of the thermally grown SiO_2 on Si because, from a mass balance consideration, a 14 nm film cannot yield 75 nm grains with the density shown in the micrographs (i.e. relatively continuous). XPS results also show that the Si to Pd ratio changes significantly after sintering. This contributes to the large grain size observed in the images on this substrate. After the second cycle of 8 h of H_2 treatment, the regenerated film shows an annealed surface where the thickness has decreased to 35 nm (fig. 4b). The microstructure displays a rather rectangular plate-like morphology and the annealed film begins to seal and leave a relatively small amount of rifts on the surface. In this case, the different activities reported in fig. 1 correspond to different microstructures.

Images obtained after the total 8 h O_2–H_2 treatment, show that the reacted Pd film (fig. 4c) exhibits 200 × 250 nm grains with an average thickness of 75 nm. Fig. 4d shows that after the second cycle O_2–H_2 treatment and reaction, there is little effect on the microstructure. The average particle size and thickness are around 200 × 200 nm and 65 nm, respectively, with slightly larger particle size distribution than the fresh film. It should be noted that in both cases of the O_2–H_2 treatment, a similar activity corresponds to similar microstructure. Yeung and Wolf [5] found that Pd films with similar microstructure yield similar reactivity, regardless of treatment history, on Pd/C catalysts using STM. Here again it is confirmed, without acquiring atomic resolution, that $Pd/SiO_2/Si$ catalyst microstructures, from first and second O_2–H_2 treatment, are very similar and again yield similar reactivity. Conversely, in the case of the H_2 treatment, Pd films with different reactivity correspond to different microstructures.

The Arrhenius parameters for 1,3-butadiene hydrogenation on the $Pd/SiO_2/Si$ film catalysts obtained at less than 20% conversion are reported in table 1a. The H_2 treated $Pd/SiO_2/Si$ fresh and regenerated film catalysts have activation energies of 10.3 and 10.1 kcal/mol respectively. The fresh and regenerated O_2 and H_2 treated $Pd/SiO_2/Si$ catalysts exhibit activation energies of 8.7 and 7.5 kcal/mol, about 2 kcal/mol lower than those of H_2 treated catalysts. Turnover numbers (TON) calculated on the basis of the geometric area are listed in table 1 at 300 K. Also listed are literature values for Pd single crystals from Massardier and coworkers [16]

Table 1
Arrhenius, kinetic, and surface roughness parameters of 1,3-butadiene hydrogenation over (a) $Pd/SiO_2/Si$, and (b) Pd/SiO_2 thin film catalyst. f denotes the surface-roughness-to-scan-area ratio

		E_a (kcal/mol)	$\ln k_0$ (mol/s gPd)	Linear regression	$T = 300$ K TON(s^{-1})	ratio, f
(a)	fresh film with 8 h H_2 treatment	10.3	12.93	0.999	53.4 (0.57)	1.13
	regenerated film with 8 h H_2 treatment	10.1	12.81	0.993	40.2 (0.42)	1.05
	fresh film with 4 h O_2 + 4 h H_2 treatment	8.7	4.04	0.999	17.6 (0.19)	1.29
	regenerated film with 4 h O_2 + 4 h H_2 treatment	7.5	2.4	0.983	3.6 (0.003)	1.14
(b)	fresh film with 8 h H_2 treatment	9.89	12.01	0.980	59.8 (0.64)	1.25
	regenerated film with 8 h H_2 treatment	9.62	11.27	0.992	77.4 (0.82)	1.07
	fresh film with 4 h O_2 + 4 h H_2 treatment	7.30	6.56	0.997	36.0 (0.38)	1.18
	regenerated film with 4 h O_2 + 4 h H_2 treatment	7.92	5.60	0.998	54.9 (0.58)	1.24
(c)	Pd(111) [a]	–	–	–	0.15	–
	Pd(110) [a]	–	–	–	1.2	–
	Pd/SiO_2 [a]	–	–	–	0.2	–

[a] Ref. [16], $T = 300$ K, $P_{H_2} = 0.7$ kPa, $P_{C_4H_6} = 0.2$ kPa.

and, in parentheses, the TON corrected to account for the differences in H_2 partial pressure between our and Massardier's study. It can be concluded that our TONs are lower than that of Pd(110) but higher than that of Pd(111) and Pd/SiO_2. Clearly the thin film catalysts are made of grains that are a mixture of several single crystal faces and their proportion varies with the pretreatment. It should be noted that the TONs listed in table 1 are reported for 300 K and are higher for the H_2 treated catalyst than for the O_2–H_2 treated catalyst. However, this trend reverses at 100°C, which agrees with the higher conversions obtained in the O_2–H_2 pretreatment.

XPS spectra of catalysts were obtained after each set of treatments and reactions. The Pd $3d_{5/2}$ and Pd $3d_{3/2}$ binding energies (BE), at 334.9 and 340.2 eV, were calibrated by using a Pd foil. Binding energy shifts due to surface charging were corrected by assigning 284.6 eV BE to the C 1s peak. The binding energies of Pd 3d, Si 2p, and O 1s are reported in table 2a. Both Si 2p peaks, from 102.2 to 103.5 eV, and O 1s peaks, from 531.53 to 532.6 eV are within the range reported for SiO_2. No surface concentrations are reported due to the presence of the ubiquitous O and C peaks which distorts the surface compositions for samples analyzed as received. While Ar sputtering can eliminate these impurities, it will alter the surface morphology and thus it was not used.

The Pd 3d binding energy initially located at 335.0 eV after evaporation, decreased by 0.2 eV after 8 h of H_2 treatment. Subsequent reaction and treatment shifted the Pd 3d peak to 335.2 eV. O_2 and H_2 treatment decreased the Pd 3d peak to 334.6 eV, and further reactions and treatment maintained the Pd 3d peak at 0.3 eV lower than the observed metallic Pd 3d binding energy. The XPS results show that the O_2–H_2 treated and reacted $Pd/SiO_2/Si$ film catalysts have consistently lower Pd binding energy than the H_2 treated and reacted catalysts. A negative Pd $3d_{5/2}$ binding energy shift was also observed by Fleish et al. [22] on Pd/La_2O_3 catalysts. The authors concluded that Pd/La_2O_3 is more electronegative than zero-valent Pd alone because electron transfer might have occurred from partially reduced oxide support on to the Pd particles.

The sintering of SiO_2 on Si complicated the imaging of the Pd supported on SiO_2/Si film catalyst. It is not possible to discern the fraction that corresponds to Pd or SiO_2 from the images. As a result, similar studies were carried out with a second SiO_2 substrate in order to isolate the effect of the substrate from the Pd microstructure.

3.2. Pd/SiO_2 THIN FILM CATALYST

Similar studies of 8 h H_2 treatment were carried out with two pieces of Pd/SiO_2 film catalysts (1.5 cm^2) while the other two pieces were treated in 4 h O_2 and 4 h H_2 at 450°C, prior to the activity measurements at 100°C with 1,3-butadiene hydrogenation.

Fig. 5 displays the activity of the fresh and regenerated Pd/SiO_2 film catalyst for the different pretreatment conditions, showing essentially the same trends as

Table 2
Elemental binding energies, in eV, for (a) $Pd/SiO_2/Si$ and (b) Pd/SiO_2 thin film catalyst. (C 1s = 284.6 eV, ΔPd is the difference in Pd 3d binding energy with respect to Pd 3d = 334.9 eV)

		Pd $3d_{5/2}$	Pd $3d_{3/2}$	Si 2p O	O 1s	ΔPd
(a)	SiO_2/Si	–	–	103.7	532.5	–
	$Pd/SiO_2/Si$	335.0	340.23	102.2	531.5	0.1
	H_2 treated $Pd/SiO_2/Si$	334.8	340.1	103.5	532.4	−0.1
	H_2 treated $Pd/SiO_2/Si$, reacted	335.0	340.3	103.3	532.3	0.1
	H_2 regenerated $Pd/SiO_2/Si$, reacted	335.2	340.5	103.3	532.6	0.3
	$O_2 + H_2$ treated $Pd/SiO_2/Si$	334.6	339.9	103.4	532.2	−0.3
	$O_2 + H_2$ treated $Pd/SiO_2/Si$, reacted	334.6	339.8	103.2	531.9	−0.3
	$O_2 + H_2$ regenerated $Pd/SiO_2/Si$ reacted	334.7	340.0	103.5	532.1	−0.2

		Pd $3d_{5/2}$	Pd $3d_{3/2}$	Si 2p	Si 2p O	O 1s	Si/SiO_2	ΔPd
(b)	SiO_2	–	–	98.3	102.4	531.1	0.30	–
	Pd/SiO_2	335.3	340.6	99.6	102.7	532.0	0.31	0.4
	H_2 treated Pd/SiO_2	334.8	340.1	99.0	103.1	532.0	0.88	−0.1
	H_2 treated Pd/SiO_2, reacted	334.8	340.1	99.2	103.4	532.3	1.62	−0.1
	H_2 regenerated Pd/SiO_2	334.9	340.2	99.2	103.5	532.2	2.25	0.1
	H_2 regenerated Pd/SiO_2, reacted	335.0	340.3	99.4	103.7	532.2	2.46	0.1
	$O_2 + H_2$ treated Pd/SiO_2	334.7	339.9	99.0	103.3	532.1	0.21	−0.2
	$O_2 + H_2$ treated Pd/SiO_2, reacted	334.6	339.8	99.0	103.2	532.1	0.44	−0.3
	$O_2 + H_2$ regenerated Pd/SiO_2	334.6	339.8	98.9	103.4	532.3	0.42	−0.3
	$O_2 + H_2$ regenerated Pd/SiO_2, reacted	334.3	339.6	98.9	103.1	531.8	0.42	−0.6

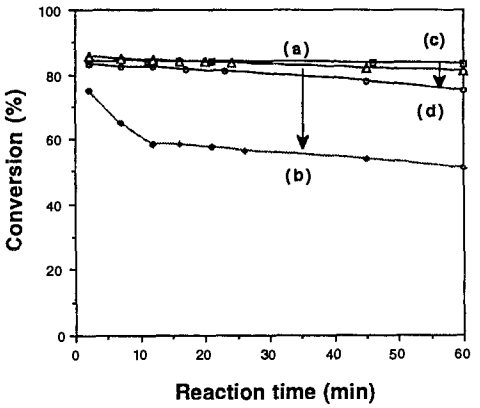

Fig. 5. The conversion of 1,3-butadiene hydrogenation over Pd/SiO_2. (a) 8 h H_2 treated fresh film, (b) 8 h H_2 regenerated film, (c) 4 h O_2 + 4 h H_2 fresh film, (d) 4 h O_2 + 4 h H_2 regenerated film.

the $Pd/SiO_2/Si$ catalysts. In this case, however, the initial conversion of both freshly treated catalysts (figs. 5a and 5c) is the same at about 85% with slight deactivation. Likewise, the Pd/SiO_2 catalyst regenerated in hydrogen (fig. 5b) shows a 35% decrease in conversion, while the one regenerated in O_2 and H_2 treatment (fig. 5d) maintains the same reactivity only with a slightly faster deactivation during 1 h of reaction.

The selectivity plots of the four major products are shown in fig. 6. The figure shows that both catalysts, with H_2, or O_2–H_2 treatment, display similar selectivity trends. The decrease of 1-butene selectivity, accompanied with increasing *n*-butane along increasing conversion, indicates that 1-butene is hydrogenated to yield *n*-butane, an effect not observed to such extent on the $Pd/SiO_2/Si$ catalysts. The increasing selectivity of cis- and trans-2-butene with conversion also suggests a separate path for the bond-shifting reaction from 1-butene and *n*-butane formation. These reaction paths were also suggested and further discussed by Pradier and coworkers [20] on Pt(100) single crystal.

AFM images, 500 × 500 nm^2, of reacted Pd/SiO_2 films are displayed in fig. 7. Closely packed 14 nm Pd grains were found on the initial Pd/SiO_2 film by STM, similar to that shown in fig. 3. The results show that the catalysts treated in H_2 and O_2–H_2 and reacted for 1 h (figs. 7a and 7b) have similar microstructures with grains scattered on the SiO_2 substrate with an average size of 75 × 65 nm for the H_2 treated and 65 × 60 nm for the O_2–H_2 treated catalysts. It should be noted that the scan area in these micrographs is 1/4 the size of those shown for the $Pd/SiO_2/Si$ catalysts (fig. 4). The difference in scan sizes arises from the significant difference in grain sizes between the two catalysts. The two microstructures observed above are very similar and again show similar reactivity. AFM images of the catalyst after the second cycle of treatment and reaction are displayed in figs. 7c and 7d. Fig. 7c shows that on the H_2 regenerated and reacted catalyst the Pd grains have coalesced and grown as large as 125 × 100 nm in size. In contrast, after the second cycle of

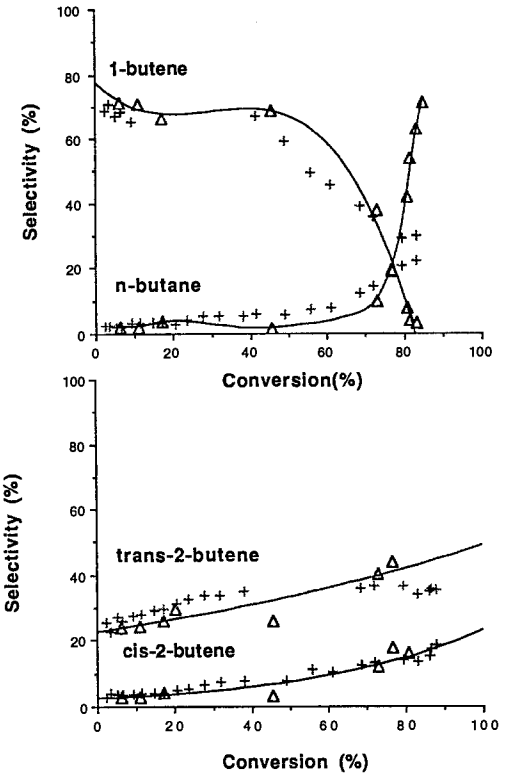

Fig. 6. The selectivity plot of 1,3-butadiene hydrogenation over Pd/SiO_2. ((△) H_2 treated sample, (+) $O_2 + H_2$ treated sample, selectivity plots of H_2 treated catalyst were interpolated.)

O_2–H_2 treatment and reaction, the catalyst is redispersed with the average particle size decreasing to 60 × 40 nm and with an average thickness of 16 nm. The shapes of the Pd grains were also studied. After two H_2 treatments and reactions (fig. 7c), the grains are more square with rounded corners which are indicative of (100) faceting. After two O_2–H_2 treatments and reactions, however, some grains show part of rounded octahedra features characteristic of (111) orientations (fig. 7d). Hence we conclude that the grain asymmetries are not the result of tips effects but rather of grain orientation. Previous STM results [9] also show that under similar pretreatments, a Pd/C catalyst shows a high percentage of asymmetric particles which did not have equilibrium shapes. The redispersion of Pt in reforming catalysts after O_2–H_2 treatment is well known although it occurs at higher temperatures and on an Al_2O_3 substrate [19]. Wang and Schmidt [13] in relation to Rh/SiO_2 particles proposed that the mechanism involves the formation of a metal oxide layer which upon reduction disperses to fine metallic particles. In fact this is an industrial procedure to redisperse Pt. It is proposed that such mechanism is also operative on these films although in this case the mechanism involves the whole grain as seen by the AFM rather than a single particle. The effect is also different insofar it also involves the absorption of H_2 on the film which may explain its effect on the larger structures of

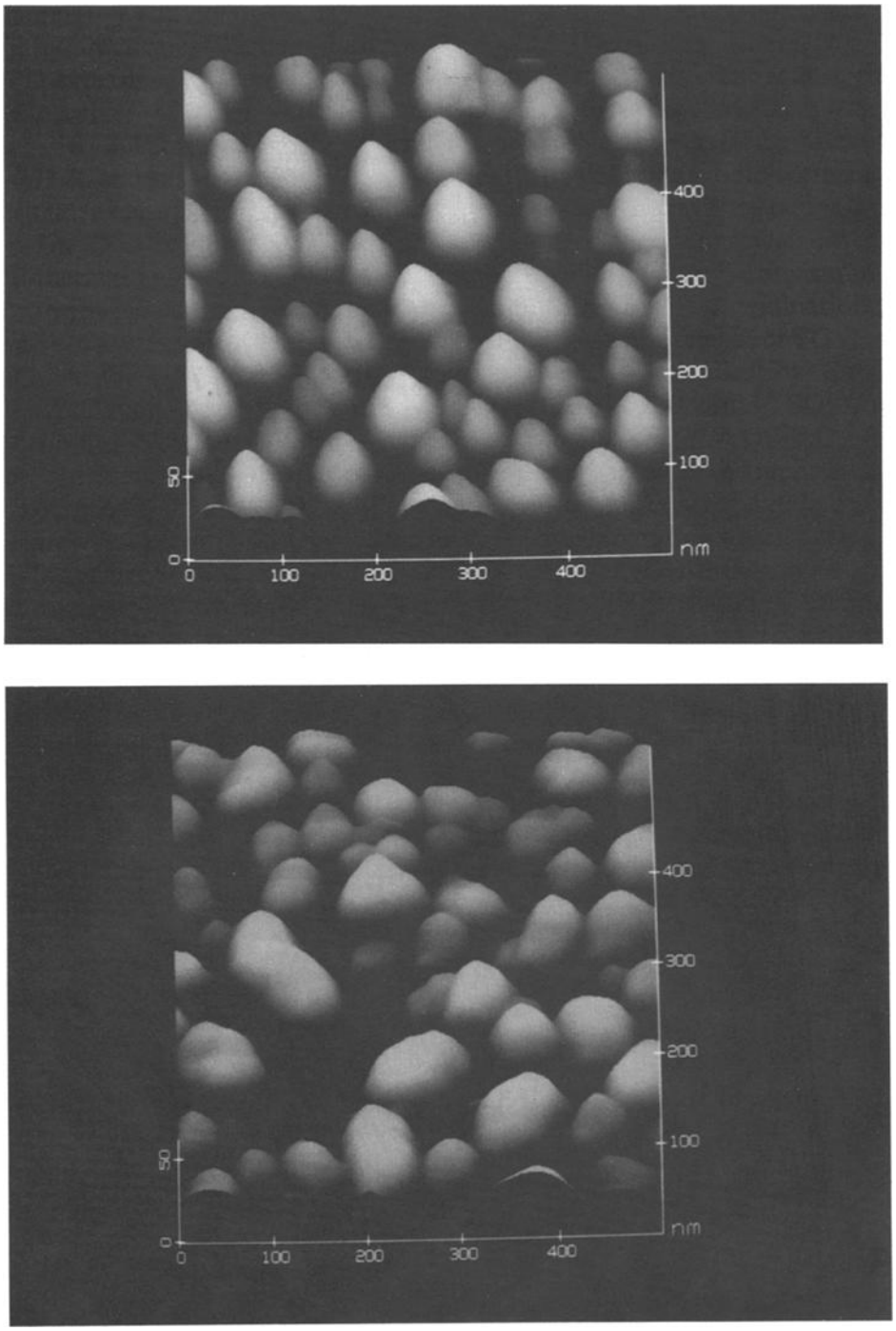

Fig. 7. AFM images of Pd/SiO_2 film catalyst after reaction. (500×500 nm^2) (a) 8 h H_2 treated fresh film, (b) 4 h O_2 + 4 h H_2 fresh film, (c) 8 h H_2 regenerated film, (d) 4 h O_2 + 4 h H_2 regenerated film.

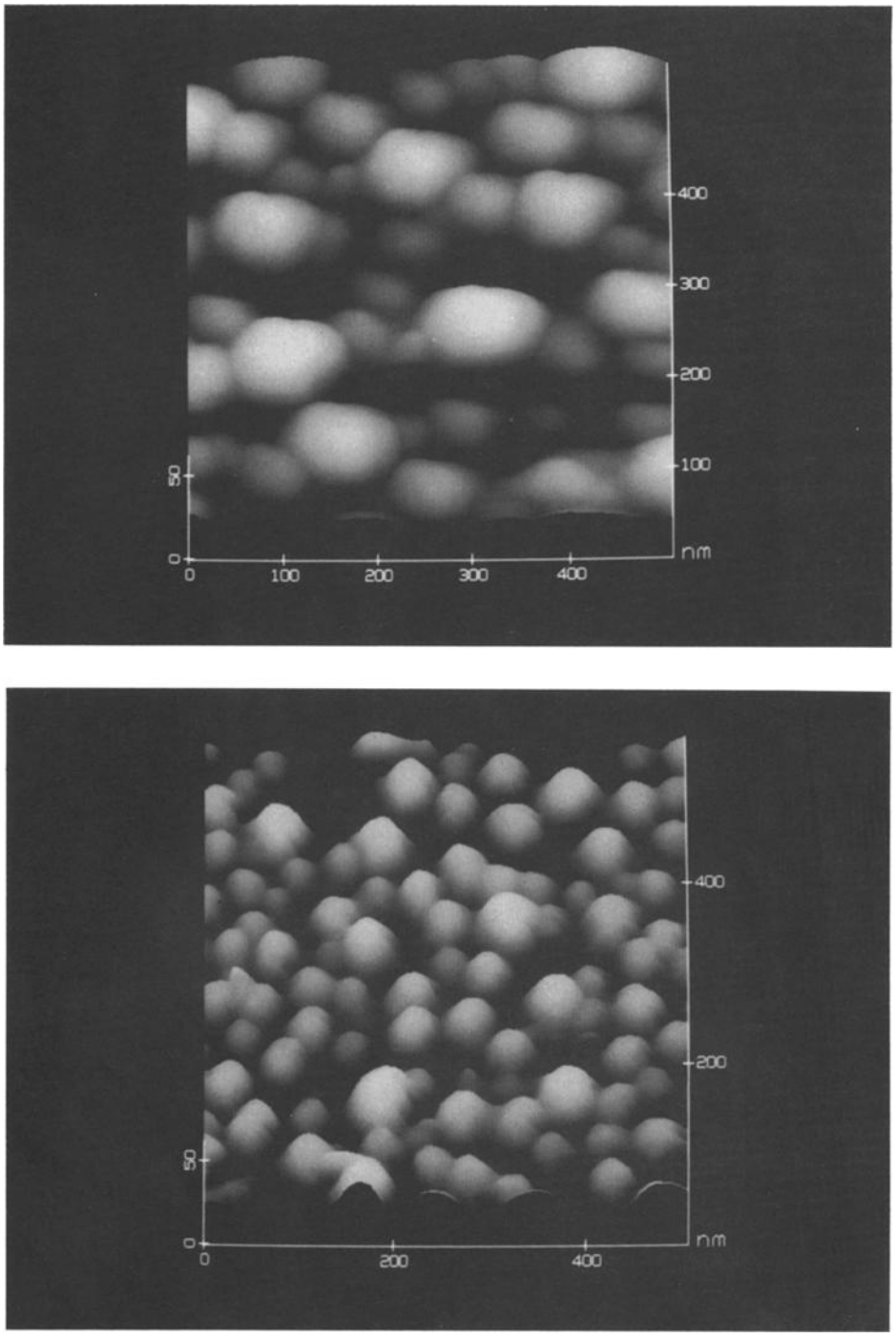

Fig. 7. Continued.

the film. It is also noted that spillover of the Pd into the substrate must also be involved since no change is seen on the substrate without Pd. Using the surface roughness program provided by Digital Instruments Inc., the surface-roughness-to-scan-area ratio, f, is listed in table 1. We found that the changes in topical area did not correspond to the differences in reactivity.

The Arrhenius parameters of both treated Pd/SiO_2 catalysts are reported in table 1b. The fresh and regenerated Pd/SiO_2 catalysts treated in hydrogen yield similar activation energies of 9.89 and 9.62 kcal/mol, whereas oxygen–hydrogen treated catalysts have activation energies of 7.30 and 7.92 kcal/mol respectively. This is a consistent 2 kcal/mol lower than that with hydrogen treatment alone, as in the case of $Pd/SiO_2/Si$ catalysts. The TONs, listed in table 1 also follow the same trends as those for the $Pd/SiO_2/Si$ catalyst when compared to the single crystal values.

The binding energies of Pd 3d, Si 2p, O 1s and C 1s transitions are reported in table 2b. From the XPS spectra, we found that the initial SiO_2 surface contains about 23% of Si. The ratios of surface Si/SiO_2 after each treatment and reaction are also reported in table 2b and are obviously higher in all four cycles of the H_2 treatments and reactions than those of the O_2–H_2 treatments and reactions. The Si 2p binding energies of Si and SiO_2 were located between 98.3 and 99.6 eV and between 102.4 and 103.7 eV respectively. The shifting of both Si 2p peaks to higher values after the deposition of Pd has also been observed by Schleich et al. [21]. O 1s peaks located between 531.1 and 532.3 eV correspond mainly to the oxygen in the SiO_2 structure. The same trends in the shifting of the Pd $3d_{5/2}$ BE were observed for the Pd/SiO_2 catalyst. Table 2b reports the differences of the Pd $3d_{5/2}$ BE after treatments and reactions with the Pd foil BE (334.9 eV). The H_2 treatment and reaction lowered the BE by 0.1 eV or less, whereas the O_2–H_2 treatment and reaction shifted it to 0.2 and 0.6 eV lower than the Pd foil after the first and second cycle respectively. Thus the O_2–H_2 treatment has not only redispersed but also reduced the Pd thin film catalyst more efficiently according to the XPS study a trend also observed in the $Pd/SiO_2/Si$ catalysts.

Comparison between the catalysts deposited on the two SiO_2 substrates indicates that the overall trends of similar activity and similar microstructure are valid in both cases. It should be noted that for the SiO_2 substrate the thickness of the Pd film remains close to the initial value (14 nm), indicating no significant changes in the morphology of the substrate, as opposed to the $Pd/SiO_2/Si$ catalyst. The sizes of the grains differ by a factor of three between the two catalysts. It is also worthwhile to note that the Pd films deposited on the SiO_2 substrate are more stable than those deposited on C previously studied in our group by STM [5]. None of the intricate surface transformations seen on the Pd/C films were observed on the Pd supported on SiO_2, which emphasizes the importance of the role of the support in stabilizing the films. Another point worth noticing is that the Si found on the Pd/SiO_2 catalyst is a result of the manufacturing process of the SiO_2 film. However, it has an effect on the grain size and on both the initial activity and the selectivity

of the catalysts. This compositional effect along with the difference in grain sizes created different sites, since the Pd/SiO_2 catalyst is more selective towards butane than 1-butene at higher conversions compared to the $Pd/SiO_2/Si$ catalyst. Ideally, we would have preferred to utilize a SiO_2 substrate containing no Si. However, the material commercially available was not pure SiO_2. On the other hand, the material we prepared was not thick enough and agglomerated given the large grain sizes.

While the AFM studies do not provide atomic resolution, it is worth emphasizing that although desirable, such level of detail is not strictly required. In fact, it is clear that even on these model catalysts there is a distribution of sites and the activity is the average obtained on each crystal terrace, edges, etc. Such detailed features are very challenging, if not impossible to characterize at atomic level in every detail. The scanning probes techniques (STM, AFM), provide a morphological characterization that appears sensitive to activity changes. In conjunction with other techniques, such as XPS, it is possible to obtain a picture of the surface that even though it is not complete, is nonetheless sufficient to gain an understanding of structural and activity relations.

4. Conclusions

The effects of pretreatment gases on Pd/SiO_2 and $Pd/SiO_2/Si$ thin film catalysts have been investigated. We found that O_2–H_2 treated Pd film catalysts have a consistent 2 kcal/mol lower activation energy, and are more reactive than the H_2 treated Pd catalysts on 1,3-butadiene hydrogenation. AFM images show that O_2 followed by H_2 treatment redisperses the Pd on the SiO_2 substrate, whereas H_2 treatment has an annealing effect on the Pd/SiO_2 film catalyst. AFM images of $Pd/SiO_2/Si$ show that on this substrate the SiO_2 agglomerates and forms grains on the surface after treatments and reactions which obstruct the imaging of Pd particles. We also found that similar Pd film microstructures correlate well with similar activities. This statement was concluded without requiring atomic resolution of the surface structure. The Pd 3d binding energy is consistently lower when the catalyst was treated with O_2–H_2 than when it was treated with H_2 alone. This indicates that O_2–H_2 treatment reduces the catalyst more efficiently than H_2 treated Pd catalyst. An increase in the Si surface composition and a decrease in grain size on Pd/SiO_2 affect the selectivity by increasing the *n*-butane formation.

Acknowledgement

Funds to purchase the equipment were provided by NSF CBT 88-06640 and the research was funded by NSF CTS 92-15339.

References

[1] G. Binnig, C.F. Quate and Ch. Gerber, Phys. Rev. Lett. 56 (1986) 930.
[2] X. Chu, L.D. Schmidt, S.G. Chen and R.T. Yang, J. Catal. 140 (1993) 543.
[3] X. Chu and L.D. Schmidt, J. Catal. 144 (1993) 77.
[4] A.M. Baro, A. Bartolome, L. Vazquez, N. Garcia, R. Reifenberger, E. Choi and R.P. Andres, Appl. Phys. Lett. 51 (1987) 159.
[5] K.L. Yeung and E.E. Wolf, J. Catal. 143 (1993) 409.
[6] K.L. Yeung and E.E. Wolf, Catal. Lett. 12 (1992) 213.
[7] M. Komiyama, S. Morita and N. Mikoshiba, J. Microscopy 152 (1988) 197.
[8] M. Komiyama, J. Kobayashi and S. Morita, J. Vac. Sci. Technol. A 8 (1990) 608.
[9] K. Yeung and E.E. Wolf, J. Vac. Sci. Technol. A 10 (1992) 651.
[10] K. Yeung and E.E. Wolf, J. Catal., accepted.
[11] C. Lee and L.D. Schmidt, J. Catal. 101 (1986) 123.
[12] C. Lee, L.D. Schmidt, J.F. Moudler and T.W. Rusch, J. Catal. 99 (1986) 472.
[13] T. Wang and L.D. Schmidt, J. Catal. 78 (1982) 306.
[14] T. Nakayama, M. Arai and Y. Nishiyama, J. Catal. 87 (1984) 108.
[15] B. Tardy, C. Noupa, C. Leclercq, J.C. Bertolini, A. Houreau, M. Treilleux, J.P. Faure and G. Nihoul, J. Catal. 129 (1991) 1.
[16] J. Massardier, J.C. Bertolini and A. Renouprez, in: *Proc. 9th Int. Congr. on Catalysis*, Vol. 3, eds. M.J. Phillips and M. Ternan (Chem. Inst. of Canada, Ottawa, 1988) p. 1222.
[17] C.-M. Pradier and Y. Berthier, J. Catal. 129 (1991) 356.
[18] V. Pitchon, M. Guenin and H. Praliaud, Appl. Catal. 63 (1990) 333.
[19] J.M. Rickard, L. Genovese, A. Moata and S. Nitsche, J. Catal. 121 (1990) 141.
[20] C.-M. Pradier, E. Margot, Y. Berthier and J. Oudar, Appl. Catal. 31 (1987) 243.
[21] B. Schleich, D. Schmeisser and W. Gopel, Surf. Sci. 191 (1987) 367.
[22] T.H. Fleisch, R.F. Hicks and A.T. Bell, J. Catal. 87 (1984) 398.